Table 2 Associations between PLNE and clinical findings ($n = 288$)

Variable	n (proportion)/mean (SD)		P	
	PLNE positive group ($n = 27$)	PLNE negative group ($n = 261$)	P-value	Adjusted P-value‡
APRI >1.5†	3 (11.1%)	4 (1.5%)	0.02	0.01§
HBV DNA (log^{10} copies/mL)	4.70 (2.97)	3.89 (2.01)	0.2	0.13¶
AST (U/L)	38.0 (33.5)	26.8 (14.5)	0.09	0.001¶
ALT (U/L)	50.1 (70.1)	28.0 (22.4)	0.11	<0.0001¶
TB (mg/dL)	0.93 (0.44)	0.93 (0.58)	0.98	-
Albumin (g/dL)	4.14 (0.29)	4.20 (0.34)	0.33	-
Platelet count ($\times 10^4/\mu L$)	18.6 (6.96)	20.6 (5.87)	0.12	0.048¶
γ-GT (U/L)	44.6 (84.1)	38.7 (110.9)	0.74	-
PT-INR	0.99 (0.09)	0.95 (0.14)	0.11	-
AFP (ng/mL)	3.22	4.68	0.15	-

†Odds ratio (95% confidence interval) for PLNE positive group was 7.85 (1.59–38.76).
‡Adjusted for sex and age at enrollment (independent variables). The dependent variables of each P-value are the items in the leftmost fields of corresponding rows (the proportion of having APRI >1.5, AST, ALT, TB and so on).
§P-value by stepwise logistic regression analysis.
¶P-value by stepwise regression analysis.
γ-GT, γ-glutamyltransferase; AFP, α-fetoprotein; ALT, alanine aminotransferase; APRI, aspartate aminotransferase-to-platelet ratio index; AST, aspartate aminotransferase; HBV, hepatitis B virus; PLNE, perihepatic lymph node enlargement; PT-INR, prothrombin time international normalized ratio; SD, standard deviation; TB, total bilirubin.

HBV or history of HCC and in 41 of 502 (8.2%) of the whole patients, and the proportion of PLNE was not significantly different between these two patient groups ($P = 0.65$, χ^2-test). In addition, in patients receiving IFN or nucleoside analog treatment and/or having HCC or its past history, PLNE was found in 7.0% patients. Thus, PLNE may be observed in as much as 10% of patients with chronic HBV infections. Then, we compared the frequency of PLNE in subjects with different backgrounds; in our previous studies, PLNE was detected in 20.0% (169/846) of patients with CHC[17] and in 1.6% (69/4234) of subjects who underwent a general health examination.[19] As shown in Figure 3, the frequency of PLNE in patients with chronic HBV infection was significantly higher than that in subjects undertaking a general health examination ($P < 0.0001$) but lower than that in CHC patients ($P < 0.0001$).

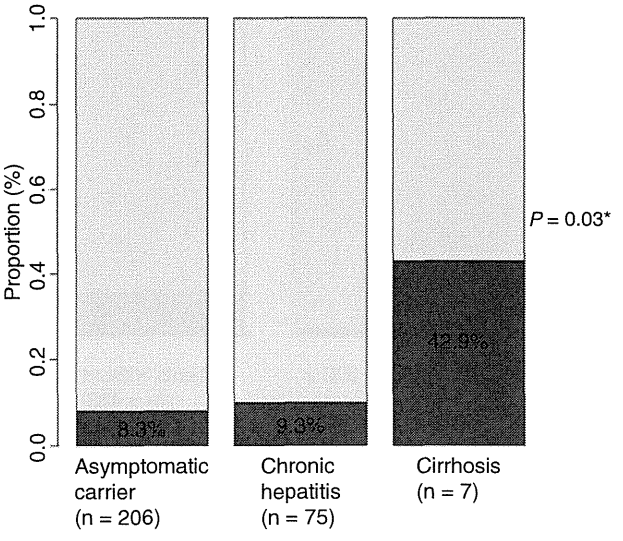

Figure 1 Bar plot of the proportion of perihepatic lymph node enlargement (PLNE) positive patients in asymptomatic carriers, patients with chronic hepatitis and patients with cirrhosis. *P-value by the Cochran–Armitage trend test. □, PLNE negative; ■, PLNE positive.

DISCUSSION

ALTHOUGH PLNE IS one of the common findings in chronic liver disease,[8–12,16,17] it has yet remained unclear how frequent PLNE would be observed or what would be the clinical significance of PLNE in patients with chronic HBV infection. In the current study, in patients without HBV treatment or HCC, PLNE was significantly associated with a higher probability of having an APRI of more than 1.5, a higher serum AST level and a higher ALT serum level. Also, a significantly increasing trend of PLNE prevalence across asymptomatic carriers, patients with chronic hepatitis and patients with

Table 3 Patient characteristics according to prevalence of HCC in the original cohort ($n = 502$)

Variable	n (proportion)/mean (SD)		P
	HCC positive group ($n = 69$)	HCC negative group ($n = 433$)	
PLNE positive	1 (1.4%)	40 (9.2%)	0.03
APRI >1.5	8 (11.6%)	14 (3.2%)	0.005
HBV DNA (log^{10} copies/mL)	1.19 (1.67)	3.00 (2.36)	<0.0001
AST (U/L)	30.4 (17.8)	28.3 (27.3)	0.40
ALT (U/L)	27.2 (19.1)	29.5 (38.1)	0.42
TB (mg/dL)	1.02 (0.45)	0.95 (0.56)	0.29
Albumin (g/dL)	4.08 (0.41)	4.20 (0.39)	0.03
Platelet count ($\times 10^4/\mu L$)	14.0 (5.41)	19.7 (6.10)	<0.0001
γ-GT (U/L)	48.8 (50.2)	40.9 (98.9)	0.31
PT-INR	1.00 (0.12)	0.98 (0.25)	0.60

γ-GT, γ-glutamyltransferase; ALT, alanine aminotransferase; APRI, aspartate aminotransferase-to-platelet ratio index; AST, aspartate aminotransferase; HBV, hepatitis B virus; HCC, hepatocellular carcinoma; PLNE, perihepatic lymph node enlargement; PT-INR, prothrombin time international normalized ratio; SD, standard deviation; TB, total bilirubin.

cirrhosis was observed, suggesting that PLNE may be associated with progress of liver fibrosis and severer hepatocellular damage in patients with chronic HBV infection. Furthermore, the frequency of PLNE in patients with chronic HBV infection was significantly lower than that in CHC patients. To the best of our knowledge, this is the first study showing the clinical significance of PLNE in chronic HBV infection.

It is well known that liver fibrosis and hepatocellular injury are associated with HCC occurrence generally in chronic liver disease.[21] Furthermore, recent evidence has revealed that serum HBV DNA level is a risk for hepatocarcinogenesis in chronic HBV infection.[22] In the current study, PLNE was associated with liver fibrosis, hepatocellular injury and serum HBV DNA level, however, PLNE was less frequently observed in patients with HCC and/or its history than in those without HCC in our original sample ($n = 502$). Although this paradoxical result is interesting, its mechanism remains to be clarified. Of note, we previously reported that PLNE was a negative risk for HCC occurrence in CHC patients.[17] Thus, the result in the present study may imply the similar association between PLNE and the development of HCC in patients with chronic liver disease in general. One probable explanation for this paradoxical result is that the presence of PLNE may reflect a stronger immune response to hepatitis virus, which could exert also an antitumor immune response.

On multivariate analysis regarding HCC prevalence and clinical parameters, lower ALT levels were significantly associated with higher prevalence of HCC. This

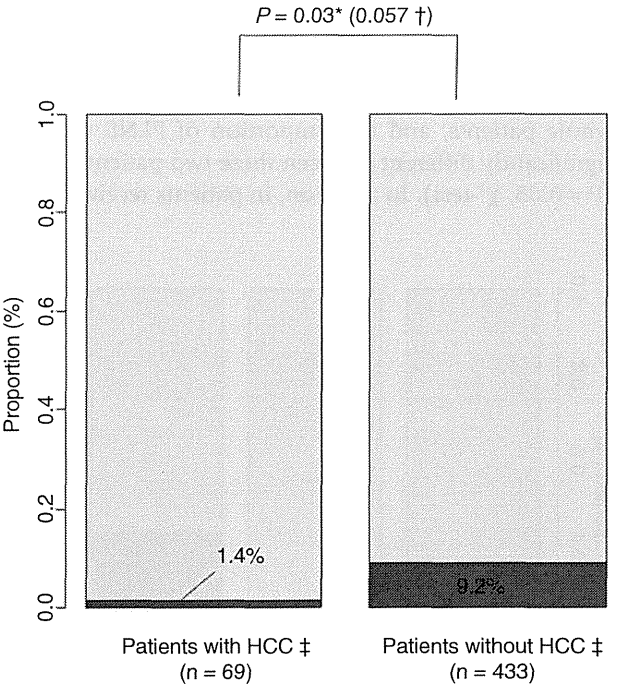

Figure 2 Bar plot of the proportion of perihepatic lymph node enlargement (PLNE) positive patients with and without hepatocellular carcinoma (HCC). **P*-value by Fisher's exact test. †*P*-value by logistic regression test (adjustment for age, sex, aspartate aminotransferase-to-platelet ratio index score, alanine aminotransferase, total bilirubin, albumin and γ-glutamyltransferase). ‡Patients receiving interferon or nucleoside analog treatment were also included. □, PLNE negative; ■, PLNE positive.

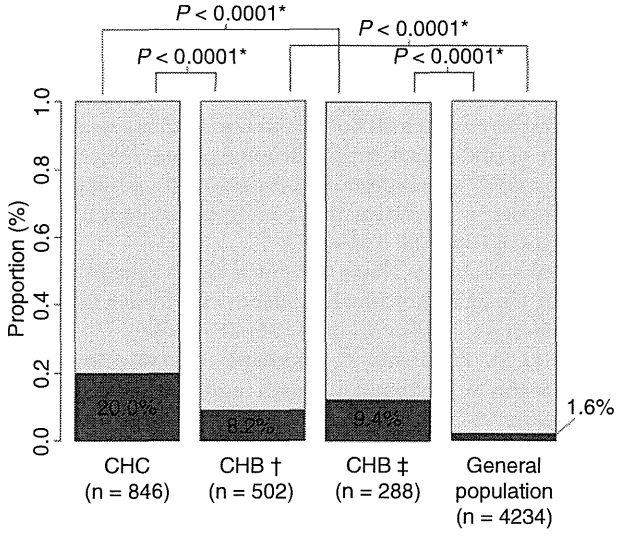

Figure 3 Bar plot of the proportion of perihepatic lymph node enlargement (PLNE) positive patients in chronic hepatitis B (CHB), chronic hepatitis C (CHC) and general health examination. **P*-value by the χ^2-test. †Total patients; ‡Patients without history of hepatocellular carcinoma or treatment for CHB. □, PLNE negative; ■, PLNE positive.

unexpected result may be explained by the treatment effect for HBV. Nucleotide analog treatment has been generally applied in symptomatic patients but not asymptomatic ones in our cohort, in which HCC occurred more frequently in these symptomatic patients. Indeed, the proportion receiving nucleotide analog treatment was higher in HCC positive patients compared with HCC negative patients (71.0% vs 33.4%, $P < 0.0001$, data not shown), which may explain the lower ALT levels in HCC positive patients. Lower HBV DNA levels in HCC positive patients compared to HCC negative patients (1.19 vs 3.00, $P < 0.0001$, Table 3) may be similarly explained by nucleotide analog treatment.

It should be noted that controversy still exists regarding whether PLNE could be associated with hepatocellular damage or liver fibrosis in patients with chronic HCV infection.[6–9,11,13,14] These results raise a possibility that the clinical significance of PLNE may be distinct regarding the association with hepatitis activity between chronic HBV infection and chronic HCV infection. The distinct PLNE frequency between chronic HBV infection and chronic HCV infection observed in the current study may be in line with this concept. Hyperplasia of regional lymph nodes are generally considered to reflect inflammatory responses in the adjacent organs. Especially in chronic HCV infection, PLNE are thought to reflect the immunological response of the host.[11] Indeed, HCV-specific IFN-γ production and proliferative response of T cells were found commonly in perihepatic lymph nodes,[23] suggesting that PLNE indicates an active host immune response in chronic hepatitis C. The humoral immune response plays an essential role in HBV and HCV infection.[24] Almost 40% of patients infected with HCV were reported to develop at least one extrahepatic manifestation during the course of the disease.[25] CHC patients were shown to be associated with mixed cryoglobulinemia, chronic thyroiditis, Sjögren's syndrome or membranoproliferative glomerulonephritis.[26–31] On another front, extrahepatic manifestations of hepatitis B were reported to be present in 1–10% of HBV-infected patients, which is lower than that of HCV-infected patients, including serum sickness-like syndrome, acute necrotizing vasculitis (polyarteritis nodosa), membranous glomerulonephritis or popular acrodermatitis of childhood (Gianotti–Crosti syndrome).[32,33] Thus, there may be an apparent incompatibility between patients with chronic HBV and HCV infection in terms of the component of immune system. The result of the present study may support this concept.

In patients not receiving IFN or nucleoside analog treatment, and those without having HCC or its past history for comparison with other background ($n = 288$) to avoid an influence of antiviral treatment or HCC occurrence, the frequency of PLNE was 9.4%. Although these patients appear to be biased toward a less severely ill patient population, the frequency of PLNE in these patients was not significantly different from that in the original 502 patients (8.2%). Of note, the frequency of PLNE in CHB patients was much lower than that in chronic hepatitis C patients, as previously reported. As suggested earlier, the different components of the immune system in patients with chronic HBV and HCV infections could explain this difference.

This study is limited by the absence of some important clinical details such as information about the histological findings of fibrosis and inflammation. Although the APRI is a useful index for the prediction of fibrosis, the limitation of this score has been reported in previous studies.[34,35] However, we also showed that the prevalence of the patients with clinically diagnosed liver cirrhosis was also significantly higher in the patients with PLNE ($P = 0.0009$), which may minimize this limitation. Another limitation to consider is the cross-sectional design of the present study, which does not allow causal inferences and limits any assumptions about the duration of the existence of any of the criteria,

such as APRI score, ALT level or HCC occurrence. Also, clinical findings at the onset of PLNE were not accessible. Moreover, for comparison of the frequency of PLNE in patients with HCC and/or its history and those without, only one HCC patient with PLNE positivity was included in the present study. Thus, the sample may not be large enough, especially for adjustment of other covariates. Further prospectively designed study with a larger sample is needed to elucidate the association between PLNE and the risk of hepatocarcinogenesis.

In conclusion, in spite of the positive association between the presence of PLNE and progressed fibrosis or higher hepatocellular injury, the presence of PLNE was negatively associated with the prevalence of HCC in patients with chronic HBV infection.

REFERENCES

1 Lavanchy D. Hepatitis B virus epidemiology, disease burden, treatment, and current and emerging prevention and control measures. *J Viral Hepat* 2004; **11**: 97–107.
2 Parkin DM. Global cancer statistics in the year 2000. *Lancet Oncol* 2001; **2**: 533–43.
3 Bosch FX, Ribes J, Diaz M, Cleries R. Primary liver cancer: worldwide incidence and trends. *Gastroenterology* 2004; **127**: S5–S16.
4 Chisari FV, Ferrari C. Hepatitis B virus immunopathogenesis. *Annu Rev Immunol* 1995; **13**: 29–60.
5 Cassani F, Zoli M, Baffoni L *et al.* Prevalence and significance of abdominal lymphadenopathy in patients with chronic liver disease: an ultrasound study. *J Clin Gastroenterol* 1990; **12**: 42–6.
6 Cassani F, Valentini P, Cataleta M *et al.* Ultrasound-detected abdominal lymphadenopathy in chronic hepatitis C: high frequency and relationship with viremia. *J Hepatol* 1997; **26**: 479–83.
7 Dietrich CF, Lee JH, Herrmann G *et al.* Enlargement of perihepatic lymph nodes in relation to liver histology and viremia in patients with chronic hepatitis C. *Hepatology* 1997; **26**: 467–72.
8 Soresi M, Carroccio A, Agate V *et al.* Evaluation by ultrasound of abdominal lymphadenopathy in chronic hepatitis C. *Am J Gastroenterol* 1999; **94**: 497–501.
9 Zhang XM, Mitchell DG, Shi H *et al.* Chronic hepatitis C activity: correlation with lymphadenopathy on MR imaging. *AJR Am J Roentgenol* 2002; **179**: 417–22.
10 del Olmo JA, Esteban JM, Maldonado L *et al.* Clinical significance of abdominal lymphadenopathy in chronic liver disease. *Ultrasound Med Biol* 2002; **28**: 297–301.
11 Muller P, Renou C, Harafa A *et al.* Lymph node enlargement within the hepatoduodenal ligament in patients with chronic hepatitis C reflects the immunological cellular response of the host. *J Hepatol* 2003; **39**: 807–13.
12 Watanabe T, Sassa T, Hiratsuka H, Hattori S, Abe A. Clinical significance of enlarged perihepatic lymph node on ultrasonography. *Eur J Gastroenterol Hepatol* 2005; **17**: 185–90.
13 Soresi M, Carroccio A, Bonfissuto G *et al.* Ultrasound detection of abdominal lymphadenomegaly in subjects with hepatitis C virus infection and persistently normal transaminases: a predictive index of liver histology severity. *J Hepatol* 1998; **28**: 544–9.
14 Tavakoli-Tabasi S, Ninan S. Clinical significance of perihepatic lymphadenopathy in patients with chronic hepatitis C infection. *Dig Dis Sci* 2011; **56**: 2137–44.
15 Soresi M, Bonfissuto G, Magliarisi C *et al.* Ultrasound detection of abdominal lymph nodes in chronic liver diseases. A retrospective analysis. *Clin Radiol* 2003; **58**: 372–7.
16 Hikita H, Enooku K, Satoh Y *et al.* Perihepatic lymph node enlargement is a negative predictor for sustained responses to pegylated interferon-alpha and ribavirin therapy for Japanese patients infected with hepatitis C virus genotype 1. *Hepatol Res* 2013; **43**: 1005–12.
17 Hikita H, Nakagawa H, Tateishi R *et al.* Perihepatic lymph node enlargement is a negative predictor of liver cancer development in chronic hepatitis C patients. *J Gastroenterol* 2013; **48**: 366–73.
18 Wai CT, Greenson JK, Fontana RJ *et al.* A simple noninvasive index can predict both significant fibrosis and cirrhosis in patients with chronic hepatitis C. *Hepatology* 2003; **38**: 518–26.
19 Gotoh H, Enooku K, Soroida Y *et al.* Perihepatic lymph node enlargement observed at a general health examination: a cross-sectional study. *Hepatol Res* 2013; **43**: 906–10.
20 Ganne-Carrie N, Ziol M, de Ledinghen V *et al.* Accuracy of liver stiffness measurement for the diagnosis of cirrhosis in patients with chronic liver diseases. *Hepatology* 2006; **44**: 1511–7.
21 Fattovich G, Stroffolini T, Zagni I, Donato F. Hepatocellular carcinoma in cirrhosis: incidence and risk factors. *Gastroenterology* 2004; **127**: S35–50.
22 Chen CJ, Yang HI, Su J *et al.* Risk of hepatocellular carcinoma across a biological gradient of serum hepatitis B virus DNA level. *JAMA* 2006; **295**: 65–73.
23 Moonka D, Milkovich KA, Rodriguez B, Abouljoud M, Lederman MM, Anthony DD. Hepatitis C. virus-specific T-cell gamma interferon and proliferative responses are more common in perihepatic lymph nodes than in peripheral blood or liver. *J Virol* 2008; **82**: 11742–8.
24 Bertoletti A, Ferrari C. Kinetics of the immune response during HBV and HCV infection. *Hepatology* 2003; **38**: 4–13.
25 Cacoub P, Renou C, Rosenthal E *et al.* Extrahepatic manifestations associated with hepatitis C virus infection. A prospective multicenter study of 321 patients. The GERMIVIC. Groupe d'Etude et de Recherche en Medecine Interne et Maladies Infectieuses sur le Virus de l'Hepatite C. *Medicine (Baltimore)* 2000; **79**: 47–56.

26 Misiani R, Bellavita P, Fenili D *et al.* Hepatitis C virus infection in patients with essential mixed cryoglobulinemia. *Ann Intern Med* 1992; **117**: 573–7.
27 Agnello V, Chung RT, Kaplan LM. A role for hepatitis C virus infection in type II cryoglobulinemia. *N Engl J Med* 1992; **327**: 1490–5.
28 Tran A, Quaranta JF, Benzaken S *et al.* High prevalence of thyroid autoantibodies in a prospective series of patients with chronic hepatitis C before interferon therapy. *Hepatology* 1993; **18**: 253–7.
29 Marazuela M, García-Buey L, González-Fernández B *et al.* Thyroid autoimmune disorders in patients with chronic hepatitis C before and during interferon-alpha therapy. *Clin Endocrinol (Oxf)* 1996; **44**: 635–42.
30 Haddad J, Deny P, Munz-Gotheil C *et al.* Lymphocytic sialadenitis of Sjogren's syndrome associated with chronic hepatitis C virus liver disease. *Lancet* 1992; **339**: 321–3.
31 Johnson RJ, Gretch DR, Yamabe H *et al.* Membranoproliferative glomerulonephritis associated with hepatitis C virus infection. *N Engl J Med* 1993; **328**: 465–70.
32 Dienstag JL. Hepatitis B as an immune complex disease. *Semin Liver Dis* 1981; **1**: 45–57.
33 Trepo C, Guillevin L. Polyarteritis nodosa and extrahepatic manifestations of HBV infection: the case against autoimmune intervention in pathogenesis. *J Autoimmun* 2001; **16**: 269–74.
34 Khan DA, Fatima Tuz Z, Khan FA, Mubarak A. Evaluation of diagnostic accuracy of APRI for prediction of fibrosis in hepatitis C patients. *J Ayub Med Coll Abbottabad* 2008; **20**: 122–6.
35 Stibbe KJ, Verveer C, Francke J *et al.* Comparison of noninvasive assessment to diagnose liver fibrosis in chronic hepatitis B and C patients. *Scand J Gastroenterol* 2011; **46**: 962–72.

Hepatology Research

Hepatology Research 2014 doi: 10.1111/hepr.12353

Original Article

An efficient system for secretory production of fibrinogen using a hepatocellular carcinoma cell line

Michinori Matsumoto,[1,2] Tomokazu Matsuura,[3] Katsuhiko Aoki,[2] Haruka Maehashi,[3] Takeo Iwamoto,[4] Kiyoshi Ohkawa,[2] Kiyotsugu Yoshida,[2] Katsuhiko Yanaga[1] and Koji Takada[2,5]

Departments of [1]Surgery, [2]Biochemistry and [3]Laboratory Medicine, [4]Core Research Facilities, and [5]Division of Biology, Department of Natural Science, The Jikei University School of Medicine, Tokyo, Japan

Aim: Despite an increasing demand, blood products are not always safe because most are derived from blood donations. One possible solution is the development and commercialization of recombinant fibrinogen, but this process remains poorly developed. This study aimed to develop an effective production system for producing risk-free fibrinogen using human hepatocellular cell lines and serum-free media.

Methods: Three human liver cancer cell lines (HepG2, FLC-4 and FLC-7) were cultivated in a serum-supplemented medium or two serum-free media (ASF104N and IS-RPMI) to compare their fibrinogen secretion abilities. Fibrinogen subunit gene expression was estimated by quantitative polymerase chain reaction. Massive fibrinogen production was induced using a 5-mL radial flow bioreactor (RFB) while monitoring glucose metabolism. Subsequently, fibrinogen's biochemical characteristics derived from these cells were analyzed.

Results: FLC-7 cell culture combined with IS-RPMI resulted in significantly better fibrinogen production (21.6 μg/10^7 cells per day). ASF104N had more positive effects on cell growth compared with IS-RPMI, whereas fibrinogen production was more efficient with IS-RPMI than with ASF104N. Changing the medium from ASF104N to IS-RPMI led to significantly increased fibrinogen gene expression and glucose consumption. In the RFB culture, the fibrinogen secretion rate of FLC-7 cells reached 0.73 μg/mL per day during a 42-day cultivation period. The subunit composition and clot formation activity of FLC-7 cell-derived fibrinogen corresponded to those of plasma fibrinogen.

Conclusion: The FLC-7 cell culture system is suitable for large-scale fibrinogen preparation production.

Key words: bioartificial liver, blood-borne pathogens, blood transfusion, fibrinogen, human cell line, radial flow bioreactor

INTRODUCTION

MORE THAN 28 million blood components are transfused each year in the USA.[1] Several transfusions are administrated to surgical and obstetric patients. Red blood cells, fresh-frozen plasma, platelets and cryoprecipitate transfusions have the potential to improve clinical outcomes in perioperative and peripartum settings. These benefits include improved tissue oxygenation and decreased bleeding. However, transfusions are not without risk because blood products can be associated with infectious disease transmission, such as hepatitis and HIV infection.[2] Blood product supply is limited and risky because most are derived from blood donations. Therefore, the development of a production method to ensure safe and plentiful supply of blood products is very important.

Fibrinogen preparations are administrated i.v. to patients with hypofibrinogenemia and are also used in combination with thrombin as a fibrin sealant during surgery. Recombinant fibrinogen production began with the cloning and subsequent expression of functional fibrinogen proteins in the early 1990s. However, the development and commercialization of fully functional recombinant fibrinogen have been difficult because of a number of complex post-translational modifications integral to its procoagulant function.[3]

Fibrinogen is a homodimer that is primarily synthesized in the liver by hepatic parenchymal cells, with each

Correspondence: Dr Michinori Matsumoto, Department of Surgery, The Jikei University School of Medicine, 3-25-8 Nishi-shinbashi, Minato-ku, Tokyo 105-8461, Japan. Email: mmatsumoto4@jikei.ac.jp
Received 9 November 2013; revision 10 April 2014; accepted 30 April 2014.

unit comprising three chains (Aα [FGA], Bβ [FGB] and γ [FGG]) encoded by different genes (*FGA*, *FGB* and *FGG*, respectively).[4] Few fibrinogen production systems using human hepatocytes or hepatoma cell lines have been reported to date,[4–7] although none have been clinically applied. The essential requirements of any cell culture system geared for effective fibrinogen production are as follows: (i) selection of a viable and highly functional hepatic cell line that can be cultivated in serum-free medium; (ii) efficient fibrinogen production maintenance; and (iii) functional fibrinogen molecule production. Functional liver cell (FLC) lines are potential candidates because they not only have liver-specific functions but also can be cultivated in serum-free medium.[8–13]

In the present study, we attempted to develop an effective fibrinogen production system that satisfied these requirements using human hepatic cell lines and serum-free medium.

METHODS

Reagents and antibodies

ALL REAGENTS WERE obtained from Sigma (St Louis, MO, USA) unless otherwise stated. The human plasma fibrinogen preparation, fibrinogen HT, was purchased from Benesis (Osaka, Japan). Peptide-N-glycosidase (PNGase F), which cleaves N-linked oligosaccharides from glycoproteins, was purchased from Life Technologies (Carlsbad, CA, USA). Primary antibodies against human fibrinogen (#A0080; Dako, Glostrup, Denmark) and human FGA (#70R-1553; Aviva Systems Biology, San Diego, CA, USA) were also used.

Cell lines and culture conditions

The FLC-4 and FLC-7 cell lines (previously known as JHH-4 and JHH-7, respectively) were initially developed from hepatocellular carcinoma cells isolated from Japanese patients, which have since been adapted to grow in serum-free medium while preserving liver-specific functions.[8,9,13] The human hepatoblastoma cell line HepG2 was purchased from the American Type Culture Collection (ATCC HB-8065; Manassas, VA, USA) and maintained in Dulbecco's modified Eagle's medium (DMEM) supplemented with 10% fetal bovine serum (FBS) (HyClone; Thermo Scientific, Logan, UT, USA) in 100-mm cell culture dishes. The FLC-4 and FLC-7 cells were maintained in ASF104N serum-free medium (Ajinomoto, Tokyo, Japan) until confluence. ASF104N is characterized by notable proliferation and exclusive use of established components that do not have an animal origin, but details on its specific components are not available because it is company confidential information. ASF104N may be modified ASF104 medium, which is a chemically defined serum-free medium that contains no peptides other than recombinant human transferrin and insulin.[14] The other serum-free medium used in this study was IS-RPMI, which comprises RPMI-1640 and HEPES buffer supplemented with small amounts of unsaturated fatty acids and inorganic trace elements, and is chemically defined as a serum-free medium without any peptides and proteins.[15,16] In certain experiments, all-trans retinoic acid (ATRA) and interleukin-6 (IL-6) (Pepro Tech, Rocky Hill, NJ, USA) were added to IS-RPMI. The harvested cell number was counted on the scheduled day using a hemocytometer.

Radial flow bioreactor culture

A radial flow bioreactor (RFB; 5 mL; Able, Tokyo, Japan) was filled with hydroxyapatite ceramic beads (diameter, 1–2 mm; pore size, <200 μm; Pentax, Tokyo, Japan).[11,17,18] FLC-7 cells were maintained in ASF104N, and $1–2 \times 10^7$ cells were transferred to RFB via an inlet tube (Fig. 1).[11] The reactor was perfused with a 3.6-mL/min medium flow velocity using a circulation pump. Cell growth and viability were monitored by measuring the ^{13}C-labeled carbon dioxide ($^{13}CO_2$) excretion rate as described below, and glucose consumption in the medium was determined using a measuring apparatus (Glutest sensor; Sanwa Kagaku Kenkyusho, Nagoya, Japan). Using the monitoring data, 100–150 mL of the medium was changed every 1–3 days through the tubing circuits (Fig. 1a). In some experiments, the medium was replaced with IS-RPMI after the cells had grown to confluence. At the end of the experiment, DNA was extracted from cells on the hydroxyapatite beads using an animal and fungi DNA preparation kit (Jena Bioscience, Jena, Germany).

$^{13}CO_2$ excretion rate

In total, 125 mg of ^{13}C-glucose was added to each liter of the serum-free media (ASF104N and IS-RPMI), both of which originally contained 2 g of glucose. The ^{13}C-labeled carbon of ^{13}C-glucose was used by the cells as $^{13}CO_2$ during glycolysis and the tricarboxylic acid cycle. Before each test initiation, the gas flowing into the reservoir was collected in sampling bags to provide a baseline sample (Otsuka Electronics, Osaka, Japan). The gas flowing out of the reservoir was collected 1, 3, 6, 9, 12, 24, 27, 30 and 33 h after medium exchange. The $^{13}CO_2$ excretion rate was measured using a POCone infrared

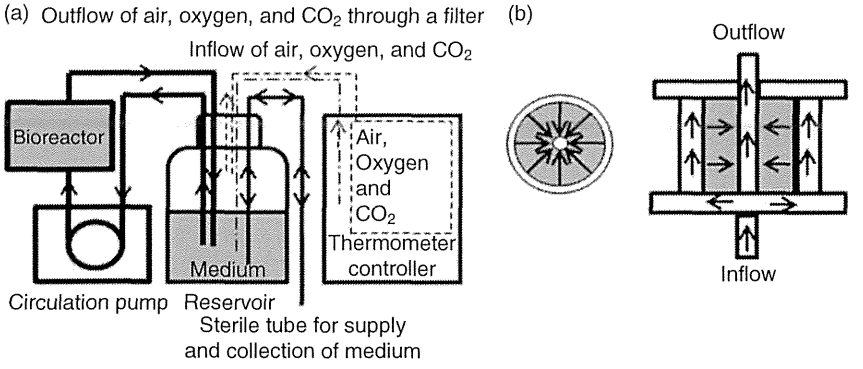

Figure 1 Schematic diagram of the radial flow bioreactor (RFB) system. The medium was circulated by a circulation pump with a medium flow velocity of 3.6 mL/min in silicone tubes connected to a reservoir medium and an RFB, which has a bed volume of 5 mL. Air was supplied to the surface of the medium in the 250-mL reservoir. The reservoir medium was stirred to ensure uniform distribution of the nutrient components. Aliquots were collected from the circulated medium through a tube (a). The medium flowed radially through the matrix bed, and the hydroxyapatite ceramic beads were packed in a vertically extended cylindrical matrix bed. The reactor creates a beneficial concentration gradient of oxygen and nutrients, while preventing excess shear stresses or the build-up of waste products (b).

spectrometer (Otsuka Electronics) and calculated using a formula similar to that used for the ^{13}C breath test.[19] $^{13}CO_2$ excretion rate:

$$\delta^{13}CO_2\ (‰) = \left(^{13}CO_2/^{12}CO_2o - {}^{13}CO_2/^{12}CO_2i\right)/\left(^{13}CO_2/^{12}CO_2i\right)\times 1000,$$

where o = outflow gas, i = inflow gas.

Fibrinogen quantification

The fibrinogen amount secreted into the media was determined using an enzyme-linked immunosorbent assay (ELISA) with normal plasma fibrinogen (E80129; Bethyl Laboratories, Montgomery, TX, USA) as a standard. The microtiter plates were coated with an appropriate dilution of goat polyclonal antibody to human fibrinogen (#55036; Cappel Research Reagents, ICN Biomedicals, Aurora, OH, USA). After blocking with phosphate-buffered saline and 1% bovine serum albumin, the standards and samples were added to the wells. The plates were then incubated at room temperature for 3 h. After multiple wash cycles with Tris-buffered saline (TBS) containing 0.05% Tween-20, appropriate dilutions of a solution of a peroxidase-conjugated antihuman fibrinogen solution (#55036), prepared using an peroxidase labeling kit-SH (Dojindo Molecular Technologies, Kumamoto, Japan), were added to the wells, and the plate was incubated at room temperature for a further 2 h. Captured enzyme-linked antibodies were detected using 3,3′,5,5′-tetramethylbenzidine substrate (#T8665; Sigma), and color development was stopped at 15 min by 1.2 N sulfuric acid addition to each well. Absorbance at 450 nm was measured using a microplate reader. The concentration in the samples was determined from standard curves and ranged 10–640 ng/mL.

RNA isolation and real-time PCR

Cellular RNA was prepared using the RNeasy mini kit (Qiagen, Hilden, Germany), and 900 ng of total RNA was reverse transcribed using ReverTra Ace (Toyobo, Osaka, Japan). Real-time polymerase chain reaction (PCR) amplification and detection were performed using the ABI step One-Plus PCR system (Applied Biosystems, South San Francisco, CA, USA). The TaqMan gene expression assay (Applied Biosystems) was used to target *FGA* (Hs00241027_m1), *FGB* (Hs00905942_m1) and *FGG* (Hs00241037_m1) and the endogenous control, the 18S ribosome (18S) sequence (Hs99999901_s1). All reactions were run in triplicate. The cycle threshold values for the genes were determined using SDS software version 2.1 (Applied Biosystems). Fibrinogen subunit gene expression is presented by the $2^{-\Delta\Delta Ct}$ value calculated by the ΔΔCt method.[20]

FLC-7 cell-derived FGA cDNA amplification and DNA sequence analysis

Human FGA cDNA from the initiation codon to the termination codon was amplified from FLC-7 cells' total RNA by PCR using the following primers: forward, 5′-CCAGCCCCACCCTTAGAAAA-3′ and reverse, 3′-AAGGAAATGCAAGGGGCCAT-5′. The PCR products

were purified using the Wizard SV gel and PCR clean-up system kit (Promega, Madison, WI, USA) and sequenced using an ABI Prism 3100 automated DNA sequencer (Applied Biosystems). Sequence similarity analyses were performed using the Basic Local Alignment Search Tool (http://blast.ncbi.nlm.nih.gov/Blast.cgi).

Cell-free protein synthesis

For cell-free FGA protein synthesis, the templates were prepared from FLC-7 cell total RNA by an overlapping PCR strategy involving two-step PCR reactions. In the first PCR round, adapter sequences were added to the 5′- and 3′-ends of the gene of interest using the following primers: forward, 5′-TAACTTTAAGAAGGAGATATACC AATGTTTTCCATGAGGATCGTCTGC-3′; and reverse, 3′-AAGGAAATGCAAGGGGCCAT-5′. In the second PCR round, a T7 promoter region was added to the first round of products using the following primers: forward, 5′-GAAATTAATACGACTCACTATAGGGAGACCACAAC GGTTTCCCTCTAGAAATAATTTTGTTTAACTTTAAGAAG GAGATATACCA-3′; and reverse, 3′-AAGGAAATGCAAG GGGCCAT-5′. The DNA template was then expressed in a cell-free transcription–translation system (PURExpress In Vitro Protein Synthesis Kit; New England BioLabs, Ipswich, MA, USA).

Electrophoretic analysis

The prepared protein samples were dissolved in sodium dodecylsulfate polyacrylamide gel electrophoresis (SDS-PAGE) sample buffer and resolved by SDS-PAGE on TGX Any kD precast gels (Bio-Rad, Hercules, CA, USA) or 4% polyacrylamide gels in Tris-glycine buffer.[21] The resolved proteins were transferred onto a polyvinylidene difluoride membrane.[22] The blotted membranes were blocked by 2-h incubation in TBS containing 0.1% Tween-20, 0.1% gelatin and 0.1% casein. Immunostaining was performed by incubating the membranes in each primary antibody at the appropriate dilution in Can Get Signal immunostain reaction solution (Toyobo) for 2 h. The membranes were then washed four times with TBS containing 0.1% Tween-20 and incubated with secondary horseradish peroxidase-conjugated antirabbit immunoglobulin Fab fragments (Nichirei, Tokyo, Japan). Immunoreactive proteins were visualized with the chemiluminescent detection reagent Immunostar LD (Wako Pure Chemical Industries, Osaka, Japan), and images were captured using a charge-coupled device camera. Prestained molecular weight standards (Bio-Rad) were used to monitor protein migration.

Fibrinogen coagulation assay

The clot formation activity in the fibrinogen samples was measured using the Clauss method[23] with a quantitative fibrinogen test kit (A&T, Kanagawa, Japan) according to the manufacturer's instructions. Briefly, a large amount of the cell culture supernatant containing fibrinogen, which had been secreted by FLC-7 cells for more than 2 months without passage, was concentrated to 1 mg/mL of fibrinogen-equivalent units by ultrafiltration using the Centricon Plus-20 centrifugal filter (EMD Millipore, Billerica, MA, USA). These samples were then incubated with thrombin reagent *in vitro* and the time to fibrin clot formation was measured to evaluate coagulation activity.

Statistical analyses

Data were presented as means ± standard deviations. The time-course data were statistically compared using two-way ANOVA with a repeated-measures design (Figs 2b,c,3a,b). Other differences in each dataset were analyzed using the Mann–Whitney *U*-test. Correlation coefficients were also calculated using a non-parametric Spearman's rank correlation coefficient. Statistical significance was set at $P < 0.05$.

RESULTS

Fibrinogen secretion from human hepatoma cell line cultures

WE COMPARED THREE human liver carcinoma cell lines (HepG2, FLC-4 and FLC-7) to determine the best one for fibrinogen secretion in culture. When DMEM supplemented with 10% FBS was used as the culture medium, the cells grew exponentially and secreted fibrinogen at 4.5–7.5 μg/10^7 cells per day (Fig. 2a). In the cultures incubated with the two serum-free media (ASF104N and IS-RPMI), the fibrinogen secretion rates were higher for FLC-7 cells than for HepG2 or FLC-4 cells (Fig. 2a). The highest fibrinogen secretion rate (21.6 μg/10^7 cells per day) was observed for FLC-7 cells combined with IS-RPMI, suggesting that this combination was most suitable to obtain a high fibrinogen yield from culture supernatants.

Serum-free medium selection

To elucidate the effects of these serum-free media on FLC-7 cell culture, we analyzed time-course changes in cell growth and fibrinogen secretion. The cells were grown to confluence in ASF104N, whereas no such cell proliferation effect was observed in cells grown in

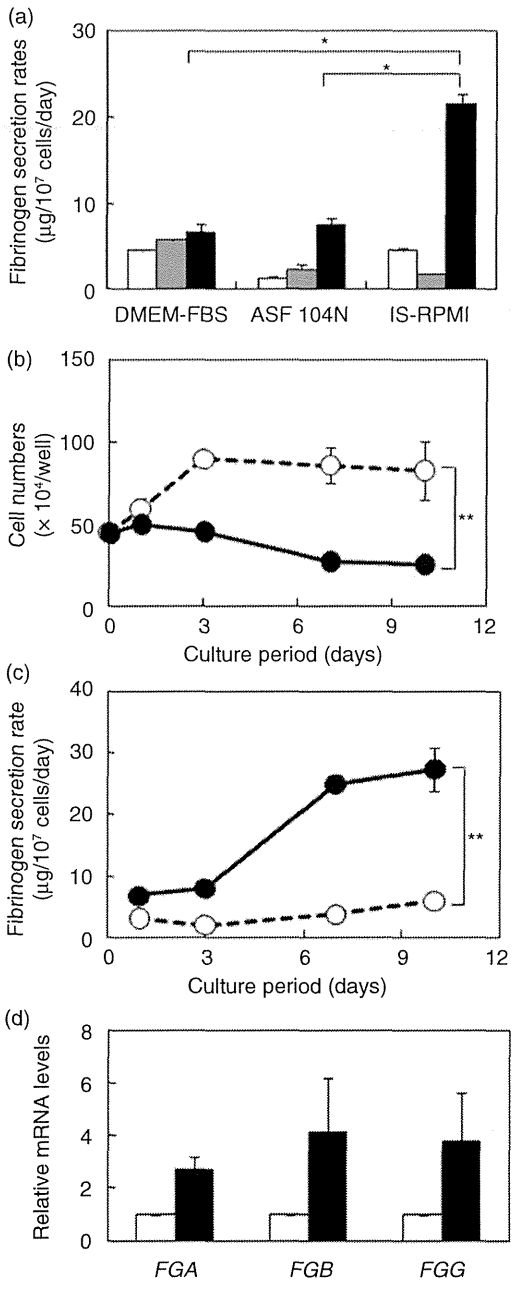

Figure 2 Fibrinogen secretion rates in monolayer culture of human hepatocellular carcinoma cell lines. Three cell lines maintained as described in the Methods section were inoculated in each well of a 24-well plate at a density of 4.5×10^5 cells/well. After 24 h of culture, the medium was removed and replaced with DMEM-FBS (Dulbecco's modified Eagle's medium supplemented 10% fasting blood sugar), ASF104N or IS-RPMI, which was replaced with the same medium every 3 days. The DMEM-FBS culture supernatants were harvested on post-inoculation day 4, and those incubated with ASF104N and IS-RPMI were harvested on day 15. Fibrinogen was quantified by enzyme-linked immunoassay. The data are expressed as mean ± standard deviation (SD) ($n = 3$ for DMEM-FBS and $n = 4$ for other media) (a). The time course of changes in cell number and fibrinogen secretion in monolayer culture of FLC-7 cells was measured. FLC-7 cells maintained in ASF104N are inoculated into each well of a 24-well plate at a density of 4.5×10^5 cells/well. After 24 h of culture, the medium was removed and replaced with ASF104N (open circles and dotted lines) or IS-RPMI (solid circles and solid lines) on day 0 and was replaced with the same medium every 3 days thereafter. Cell numbers (b) and fibrinogen secretion rates are expressed as the mean ± SD ($n = 4$ for each group) (c). The expression levels of each fibrinogen gene in FLC-7 cell culture incubated in the two serum-free media was compared. Gene expression levels were normalized using 18S as an internal control. Fold changes in mRNA for each chain (*FGA*, *FGB* and *FGG*) in IS-RPMI (solid bars) and ASF104N (open bars) were calculated using the $2^{-\Delta\Delta Ct}$ method and expressed as mean ± SD ($n = 3$) (d). * and ** represent $P < 0.05$ and $P < 0.0001$, respectively. (a) □, HepG2; ▨, FLC-4; ■, FLC-7; (b,c) ----, ASF 104N; ——, IS-RPMI; (d) □, ASF 104N; ■, IS-RPMI.

IS-RPMI (Fig. 2b). However, the fibrinogen secretion rate was greatly enhanced when ASF104N was replaced with IS-RPMI. This augmentative IS-RPMI effect was continuously observed over all experimental periods (Fig. 2c). These results indicate that IS-RPMI is a suitable medium for fibrinogen secretion, but not cell growth, and that these serum-free media should be complementarily used to ensure efficient fibrinogen production from FLC-7 cells.

IS-RPMI effects on fibrinogen chain-encoding transcription levels

The fibrinogen production pathway comprises several steps, including transcription, translation and post-translational processes for each chain. Steady-state mRNA levels of the fibrinogen chains in the FLC-7 cells were several times higher in the cultures incubated with IS-RPMI than in those incubated with ASF104N (Fig. 2d), indicating that the IS-RPMI can induce fibrinogen chain-encoding gene expression.

Fibrinogen production and glucose metabolism in RFB

To develop a semi-large scale fibrinogen production system, we scaled up FLC-7 cell culture using RFB and

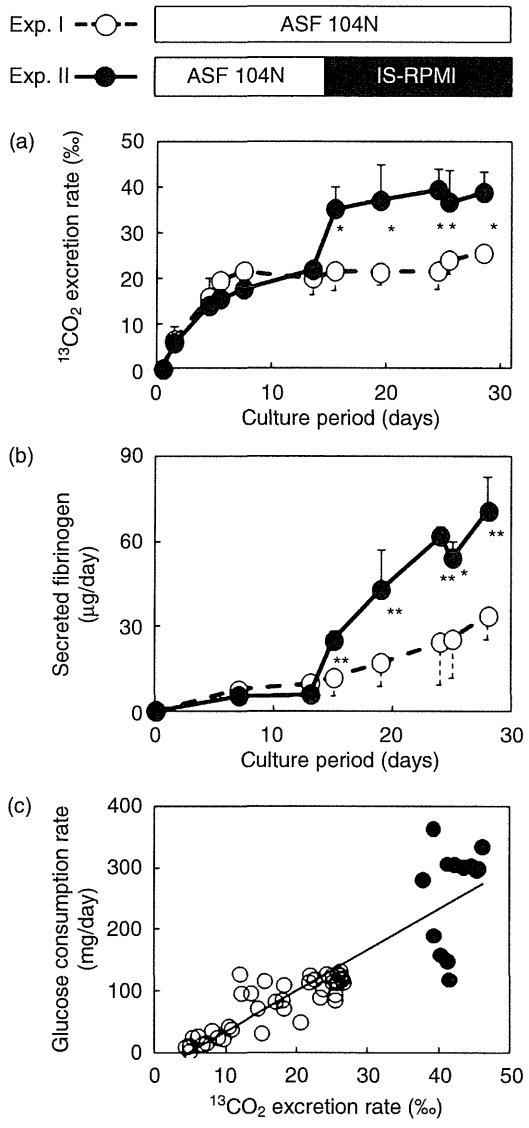

Figure 3 Time course of changes in the $^{13}CO_2$ excretion rate and fibrinogen secretion, and correlation of $^{13}CO_2$ excretion and glucose consumption in radial flow bioreactor (RFB) cultures of FLC-7 cells. FLC-7 cells maintained in ASF104N were inoculated into two 5-mL RFB at a cell density of 1.0×10^7 cells. One group, which was employed for experiment I (Exp. I, open circles and dotted lines), was cultured with ASF104N throughout the entire culture period. The other group, which was used in experiment II (Exp. II, solid circles and solid lines), was cultivated with ASF104N for 14 days and IS-RPMI for the remaining period. Small aliquots of each circulating medium were collected at appropriate intervals, and the $^{13}CO_2$ excretion rate (‰) (a) and levels of secreted fibrinogen (b) were determined in these samples ($n = 3$ for each group). While both $^{13}CO_2$ excretion rate and levels of secreted fibrinogen in the Exp. II group were not significantly different from those in the Exp. I group before the medium change ($P = 0.5017$ and $P = 0.3856$, respectively), those after the medium change were significantly higher in Exp. II groups than those in the Exp. I groups ($P = 0.0135$ and $P = 0.0094$, respectively). * and ** represent $P < 0.05$ and $P < 0.01$, respectively. FLC-7 cells were cultured in an RFB as shown in Figure 1, and small aliquots of the circulating media, ASF104N (open circles) and IS-RPMI (solid circles), were collected at appropriate intervals. The $^{13}CO_2$ excretion rate (‰) and levels of secreted fibrinogen in these samples ($n = 54$) were determined and plotted against each other. Spearman's correlation coefficient was 0.7941, which was statistically significant ($P < 0.0001$) (c).

compared two RFB culture series (Fig. 3). When FLC-7 cells were maintained in ASF104N for the entire 4-week culture period (experiment [Exp.] I), the $^{13}CO_2$ excretion rate was approximately 20‰ by day 5 and remained constant for the remaining period, suggesting that this value is indicative of the maximal cell density in RFB. In another experimental series (Exp. II), after a 13-day FLC-7 cell cultivation, the $^{13}CO_2$ excretion rate also reached approximately 20‰, following which it significantly increased to approximately 40‰ when the medium was replaced with IS-RPMI (Fig. 3a, $P = 0.0135$). In addition, the $^{13}CO_2$ excretion rate was significantly correlated with glucose consumption in the RFB cultures (Fig. 3b). At the end of the experiments, the attained fibrinogen secretion level was significantly higher in Exp. II than that in Exp. I (21.1 ± 5.0 vs 10.8 ± 1.4 μg/mg of DNA/day, respectively; $P = 0.0495$) while the DNA content in RFB of Exp. II and I were almost equal (3.4 ± 0.4 vs 3.1 ± 0.5 mg, respectively; $P = 0.2752$), indicating that the IS-RPMI also significantly stimulated fibrinogen secretion in the RFB cultures (Fig. 3b, $P = 0.0094$). In an additional experiment conducted under the same conditions as those used in Exp. II (Fig. 3), except that the initial cell number was 2.0×10^7 cells, we confirmed that IS-RPMI increased fibrinogen production to 0.73 μg/mL per day (109.5 μg/day) after a 42-day cultivation. From these results, it is evident that RFB culture of FLC-7 cells effectively produced human fibrinogen and that IS-RPMI more effectively promoted fibrinogen secretion compared with ASF104N, which is capable of maintaining FLC-7 cells in RFB.

Molecular features of FLC-7 cell-derived fibrinogen

The culture supernatants of the FLC-7 cells (FLC-7-CS) and fibrinogen product (fibrinogen HT), both of which contained the same amount of fibrinogen as estimated by ELISA, were analyzed by western blotting with whole anti-fibrinogen molecules and anti-FGA. Under non-reducing conditions, FLC-7-CS and fibrinogen HT showed strong but diffuse bands of similar intensity and relative molecular masses of 380 and 340 kDa (bands a and b in Fig. 4a), respectively, suggesting heterogeneous fibrinogen molecules. When these samples were reduced to dissociate disulfide bonds, each fibrinogen band was divided into three groups, bands c (69 kDa), e (54 kDa) and f (48 kDa) for FLC-7-CS or bands d (66 kDa), e and f for fibrinogen HT (lanes 1, 2 and 3, respectively, in Fig. 4b). Bands c and d were immunoreactive to anti-FGA, thus corresponding to FGA (lanes 4, 5 and 6 in Fig. 4b). Bands e and f were identified as FGB and FGG, respectively, according to their estimated sizes. These results indicate that FLC-7 cell-secreted fibrinogen comprises the same three chains (FGA, FGB and FGG) as plasma fibrinogen, although each FGA chain size differed slightly.

The FLC-7-CS and fibrinogen HT were then treated with glycopeptidase-F to remove N-linked carbohydrates from the glycoproteins and analyzed by western blotting. This led to a shift in FGB and FGG band mobility in both samples (Fig. 4c), indicating N-glycosylation. In contrast, FGA band mobility remained unchanged in both samples (Fig. 4c,d). Therefore, the glycosylation features of the FLC-7 cell-derived fibrinogen chains were identical to those of plasma fibrinogen.

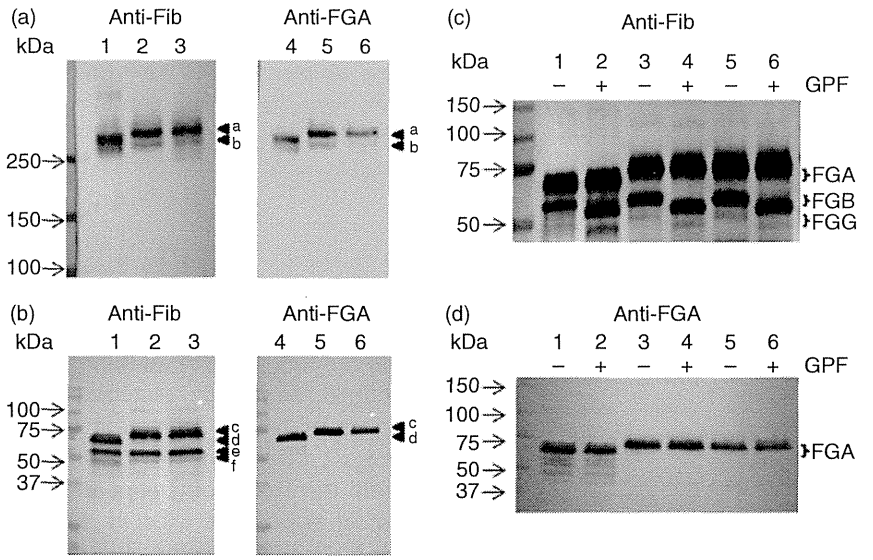

Figure 4 Western blot analysis of fibrinogen from the FLC-7 cell cultures. Samples containing 1 ng of fibrinogen each were resolved by sodium dodecylsulfate polyacrylamide gel electrophoresis using 4% polyacrylamide gels under non-reducing conditions (a). Other samples containing 2 ng of fibrinogen each were resolved using TGX Any kD precast gels under reducing conditions (b). The blots in lanes 1–3 and 4–6 were immunostained with antibodies against human fibrinogen (anti-Fib) and the N-terminus of human FGA (anti-FGA), respectively. Lanes 1 and 4, fibrinogen HT; lanes 2 and 5, culture supernatants of FLC-7 cells (FLC-7-CS) cultured as a monolayer in IS-RPMI; lanes 3 and 6, FLC-7-CS from the 5-mL radial flow bioreactor (RFB) culture. The arrowheads in (a) and (b) indicate the main bands observed in FLC-7-CS and fibrinogen HT, respectively. The arrow-heads in (c–f) correspond to FGA from FLC-7-CS, FGA of fibrinogen HT, FGB and FGG, respectively. Treatment with glycopeptidase-F was used to compare the N-linked glycosylation of plasma fibrinogen with that of FLC-7 cells. Samples containing 4 ng of fibrinogen were treated with (+) or without (–) glycopeptidase F (GPF) and resolved using TGX Any kD precast gels under reducing conditions. Blots were immunostained with antibodies against human fibrinogen (c) and the N-terminus of human FGA (d). Lanes 1 and 2, fibrinogen HT; lanes 3 and 4, culture supernatants of FLC-7 cells (FLC-7-CS) cultured as a monolayer in IS-RPMI; lanes 5 and 6, FLC-7-CS from the 5-mL RFB culture.

FLC-7 cell-derived FGA analysis by cDNA sequencing and cell-free protein translation

To identify mobility differences between fibrinogen HT FGA and FLC-7 cell-derived FGA, the FLC-7 cell-derived FGA cDNA nucleotide sequence was determined; it was completely identical to the coding sequence of human FGA deposited in the National Center for Biotechnology Information (NM_021871.2).

The *in vitro* translation product of FLC-7 cell-derived FGA cDNA was then analyzed by western blotting (Fig. 5). The electrophoretic mobility of the cDNA product (lane 4) was almost the same as that of FGA in FLC-7-CS (lanes 2 and 3, respectively). However, fibrinogen HT FGA (lane 1) migrated faster than the cDNA product. These results indicate that the fibrinogen HT FGA, derived from human plasma fibrinogen, may be truncated after translation or secretion.

FLC-7 cell-derived fibrinogen coagulation activity

A fibrinogen-rich fraction was prepared from the FLC-7-CS by ultrafiltration and was used to evaluate coagulation activity. The fibrinogen-rich fraction's clotting, determined by the Clauss method, was not significantly different from that of fibrinogen HT (24.8 ± 4.0 vs 30.1 ± 3.2 s, $P = 0.0782$ in Table 1), indicating that FLC-7-CS is a potential source material for biologically active fibrinogen.

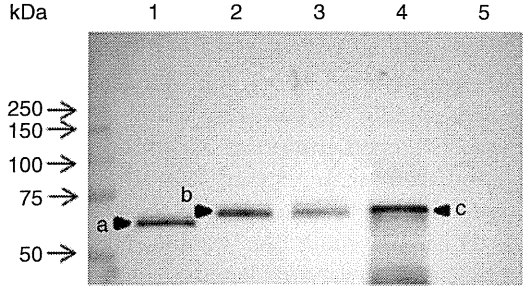

Figure 5 Comparison of FGA-immunoreactive proteins obtained from FLC-7 cell cultures with those obtained from the cell-free translation system using FGA cDNA. FGA cDNA prepared from FLC-7 cells was used as the template for protein synthesis using a cell-free transcription and translation system. The product obtained and other fibrinogen samples containing 1 ng of fibrinogen each were resolved using a TGX Any kD precast gel under reducing conditions. The blots were immunostained with antibodies against the N-terminus of human FGA (E). Lane 1, fibrinogen HT; lane 2, culture supernatants of FLC-7 cells (FLC-7-CS) cultured as a monolayer in IS-RPMI; lane 3, FLC-7-CS from the 5-mL radial flow bioreactor (RFB); lane 4, the cell-free synthesis product obtained using FGA cDNA from FLC-7 cells; lane 5, the reaction mixture of the cell-free synthesis without FGA cDNA (negative control).

Table 1 Clot formation time (s) for the fibrinogen preparations

Sample no.	Fibrinogen HT	FLC-7 fibrinogen
1	29.2	28.0
2	21.6	26.2
3	26.4	30.9
4	20.6	35.2
5	29.1	28.5
6	21.6	32.0
Clot formation time (s)	24.8 ± 4.0	30.1 ± 3.2

Coagulation activity was measured using a procedure based on the Clauss method. The fibrinogen concentrations derived from the FLC-7 cells (fibrinogen-FLC-7) and plasma (fibrinogen HT) were adjusted to 1 mg/mL. Subsequently, an excess of thrombin was added to the samples and clot formation time was measured. The clot formation times are expressed as means ± standard deviations. No significant between-group difference was observed ($P = 0.0782$).

Substances that stimulate fibrinogen secretion

In an attempt to obtain more fibrinogen from FLC-7-CS, we tested several additives in monolayer culture cells in IS-RPMI and found that supplemental ATRA and/or IL-6 brought about a significant increase in fibrinogen levels in the culture supernatants (Fig. 6). Although this effect was more prominent for IL-6 than for ATRA, the combination of both was the most effective. Therefore, chemical mediators such as IL-6 and ATRA may be useful to improve the fibrinogen production by FLC-7 cells.

DISCUSSION

THE HUMAN HEPATOBLASTOMA cell line HepG2 exhibits many normal hepatocyte characteristics.[24,25] HepG2 cells cultured in DMEM with 10% FBS are appropriate to investigate the mechanisms underlying fibrinogen production, assembly and secretion.[4–7] In this study, the fibrinogen secretion rate of HepG2 cells incubated in DMEM with 10% FBS (4.5 ± 0.1 μg/day per 10^7 cells) was almost the same as that reported in a previous study.[26] However, serum-supplemented medium was not suitable for this study because of the cost and risk of adventitious agent transmission from animal sera.[2,3]

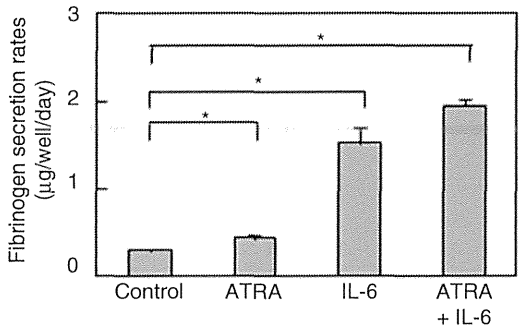

Figure 6 Effects of all-trans retinoic acid (ATRA) and interleukin-6 (IL-6) on fibrinogen secretion in FLC-7 cell cultures. FLC-7 cells were inoculated into each well of a 24-well plate at a density of 4.5×10^5 cells/well. After 24 h of culture, the medium was removed and replaced with IS-RPMI containing 1 μM of ATRA and/or 50 ng/mL of IL-6. The culture supernatants were harvested the following day. Fibrinogen was quantified by enzyme-linked immunoassay. Calculated data are expressed as mean ± standard deviation ($n = 6$ for each group). * represents $P < 0.01$.

FLC-4 and FLC-7 cell lines developed from hepatocellular carcinoma specimens from Japanese patients have been adapted to grow in serum-free medium, thus preserving their liver-specific functions.[8,9,13] Although several studies have examined FLC-4 and FLC-7 cell function,[12,27] we showed here, effective fibrinogen production by FLC-7 cells using an RFB system for the first time as per our knowledge. With regard to potential viral hepatitis infection, whole hepatitis B (HB) virus DNA is not integrated into FLC-7 cells. In addition, HB surface, HB e- and HB core antigens were undetectable in the cells and the supernatant by an enzyme immunoassay.[8] Also, hepatitis C virus RNA was not detected by PCR in frozen tissue obtained from the patient from whom the FLC-7 cell line was derived (data not shown). The Japanese Collection of Research Bioresources Cell Bank showed that other viruses such as HIV, human T-cell lymphotropic virus type (HTLV)-1 and -2 were also not detected in FLC-7 cells.[28] Therefore, FLC-7 cells do not appear to be infected with the hepatitis B, C viruses, HIV, HTLV-1 and -2.

The two serum-free media, ASF104N and IS-RPMI, showed contrasting results. The former is apparently more effective than the latter with regard to FLC-7 cell proliferation, although the latter is much more effective than the former with regard to fibrinogen secretion and increased glucose consumption. In addition, the cell viability in IS-RPMI was maintained for at least more than 1 month in RFB culture and for more than 2 months without passage in monolayer culture (data not shown). The appropriate combination of the two serum-free media is the key to effective fibrinogen production. Several speculative mechanisms for this phenomenon are possible. One mechanism may include a switch from growth to differentiation because well-differentiated hepatocytes stop growing and maintain high gene expression levels and albumin, transferrin and fibrinogen secretion rates.[29] Another possibility is an acute phase-like response, during which plasma fibrinogen levels can be greatly increased;[4,30] the acute phase response increases glucose consumption and causes hypermetabolism.[31] In addition, the levels of hypoxia-inducible factor-1α (HIF-1α) in FLC-7 cells, estimated by western blotting, were increased by the culture with IS-RPMI (data not shown). HIF-1α may upregulate glucose uptake and lead to increase of $^{13}CO_2$ excretion rate in the IS-RPMI groups because the activation of the HIF-1α pathway leads to augmented glucose transporter 1 (GLUT1) gene expression.[32] However, the precise mechanism by which the simple serum-free medium IS-RPMI drives these phenomena remains unclear, warranting further examinations. On the other hand, IL-6 and ATRA reportedly increased fibrinogen gene expression and secretion in normal hepatocytes and HepG2 cells.[5,30] These substances showed the similar effects on FLC-7 cells cultured in IS-RPMI (Fig. 6), which suggested that IS-RPMI, IL-6 and ATRA had the augmentative effects on fibrinogen production by the independent mechanisms.

Plasma fibrinogen comprises a heterogeneous molecule population with varying FGA chain lengths.[33] Although FGA originally comprises 644 amino acids with a 69 757-Da molecular weight (NP_068657.1), FGA molecules of varying lengths share a common amino terminus, although they differ at their carboxyl termini, which is highly susceptible to processing by some plasma proteases.[33,34] Different FGA band mobility observed in fibrinogen HT and FLC-7-CS (Figs 4,5) is caused by carboxyl termini processing because the cell-free system reconstituted from the purified components necessary for *Escherichia coli* translation failed to induce post-translational modifications. Regarding the cell-free system, the slightly different electrophoretic mobility between the translated products and FGA in FLC-7-CS (Fig. 5) is due to the presence of a 19-amino acid signal sequence of human FGA (NP_068657.1).[35,36]

Three-dimensional cell culture using RFB has many advantages in terms of drug production and synthesis because it can maintain natal morphology and cell

function and can achieve conditions closely resembling the *in vivo* state for extended periods.[3,11,37] To assess productivity, the fibrinogen production system in this study was compared with others to produce recombinant fibrinogen.[38-41] Recombinant fibrinogen production rates for baby hamster kidney (BHK) cells in DMEM with 5% FBS,[38] African green monkey kidney (COS-1) cells in Iscove's medium with 10% FBS,[39] Chinese hamster ovary (CHO) cells in DMEM with 5% FBS,[40] and *Pichia pastoris* in YPD[41] range 1–2 μg/mL per day. On the other hand, that for the FLC-7 cell culture using RFB was 0.73 μg/mL per day, comparable to that for the previously reported recombinant fibrinogen production systems. Furthermore, the culture system developed in this study was more efficient for several reasons. First, this culture system guarantees the highly safe products because it employs the serum-free media and the cells without the pathogen that causes hepatitis or other infections. Second, IS-RPMI, the optimal medium for this system, is highly cost-effective. Third, the system using RFB is easy to scale up for mass production. Furthermore, we expect much greater fibrinogen production in combination with appropriate additives such as ATRA and/or IL-6. Our study also has several limitations. First, we could not confirm the safety of FLC-7 fibrinogen administration to humans, by glycan analyses, which play important roles in antigen determination.[42] Second, we were unable to analyze clot stability, including not only viscoelastic but also fibrinolytic properties.[43] Further assessment from multiple perspectives is essential to assess fibrinogen function for clinical use.

We conclude that FLC-7 cell culture in RFB combined with the two serum-free media has considerable advantages in terms of fibrinogen production relative to other techniques. Further studies are required to assess the safety and efficacy of this fibrinogen preparation system for clinical application.

ACKNOWLEDGMENTS

THIS WORK WAS supported by a Grant-in-Aid from The Japan Health Sciences Foundation (Research on Publicly Essential Drugs and Medical Devices, KHC1202).

REFERENCES

1 Sullivan MT, Cotten R, Read EJ *et al.* Blood collection and transfusion in the United States in 2001. *Transfusion* 2007; **47**: 385–94.
2 Satake M. Infectious risks associated with the transfusion of blood components and pathogen inactivation in Japan. *Int J Hematol* 2004; **80**: 306–10.
3 Wurm FM. Production of recombinant protein therapeutics in cultivated mammalian cells. *Nat Biotechnol* 2004; **22**: 1393–8.
4 Redman CM, Xia H. Fibrinogen biosynthesis. Assembly, intracellular degradation, and association with lipid synthesis and secretion. *Ann N Y Acad Sci* 2001; **936**: 480–95.
5 Nicodeme E, Nicaud M, Issandou M. Retinoids stimulate fibrinogen production both in vitro (hepatocytes) and in vivo. Induction requires activation of the retinoid X receptor. *Arterioscler Thromb Vasc Biol* 1995; **15**: 1660–7.
6 Koj A, Korzus E, Baumann H *et al.* Regulation of synthesis of some proteinase inhibitors in human hepatoma cells HepG2 by cytokines, hepatocyte growth factor and retinoic acid. *Biol Chem Hoppe Seyler* 1993; **374**: 193–201.
7 Kasza A, Bugno M, Koj A. Long-term culture of HepG2 hepatoma cells as a model for liver acute phase response during chronic inflammation. Effects of interleukin-6, dexamethasone and retinoic acid. *Biol Chem Hoppe Seyler* 1994; **375**: 779–83.
8 Fujise K, Nagamori S, Hasumura S *et al.* Integration of hepatitis B virus DNA into cells of six established human hepatocellular carcinoma cell lines. *Hepatogastroenterology* 1990; **37**: 457–60.
9 Homma S, Nagamori S, Fujise K *et al.* [Establishment and characterization of a human hepatocellular carcinoma cell line JHH-7 producing alpha -fetoprotein and carcinoembryonic antigen–changes in secretion of AFP and CEA from JHH-7 cells after heat treatment]. *Hum Cell* 1990; **3**: 152–7.
10 Iwahori T, Matsuura T, Maehashi H *et al.* CYP3A4 inducible model for in vitro analysis of human drug metabolism using a bioartificial liver. *Hepatology* 2003; **37**: 665–73.
11 Kawada M, Nagamori S, Aizaki H *et al.* Massive culture of human liver cancer cells in a newly developed radial flow bioreactor system: ultrafine structure of functionally enhanced hepatocarcinoma cell lines. *In Vitro Cell Dev Biol Anim* 1998; **34**: 109–15.
12 Laurent T, Murase D, Tsukioka S *et al.* A novel human hepatoma cell line, FLC-4, exhibits highly enhanced liver differentiation functions through the three-dimensional cell shape. *J Cell Physiol* 2012; **227**: 2898–906.
13 Hasumura S, Sujino H, Nagamori S *et al.* [Establishment and characterization of a human hepatocellular carcinoma cell line JHH-4]. *Hum Cell* 1988; **1**: 98–100.
14 Fukaya K, Asahi S, Nagamori S *et al.* Establishment of a human hepatocyte line (OUMS-29) having CYP 1A1 and 1A2 activities from fetal liver tissue by transfection of SV40 LT. *In Vitro Cell Dev Biol Anim* 2001; **37**: 266–9.
15 Nakabayashi H, Taketa K, Miyano K *et al.* Growth of human hepatoma cells lines with differentiated functions in chemically defined medium. *Cancer Res* 1982; **42**: 3858–63.

16 Nakabayashi H, Taketa K, Yamane T *et al.* Phenotypical stability of a human hepatoma cell line, HuH-7, in long-term culture with chemically defined medium. *Gann* 1984; **75**: 151–8.
17 Matsuura T, Kawada M, Hasumura S *et al.* High density culture of immortalized liver endothelial cells in the radial-flow bioreactor in the development of an artificial liver. *Int J Artif Organs* 1998; **21**: 229–34.
18 Nagamori S, Hasumura S, Matsuura T *et al.* Developments in bioartificial liver research: concepts, performance, and applications. *J Gastroenterol* 2000; **35**: 493–503.
19 Schoeller DA, Klein PD, Watkins JB *et al.* 13C abundances of nutrients and the effect of variations in 13C isotopic abundances of test meals formulated for 13CO2 breath tests. *Am J Clin Nutr* 1980; **33**: 2375–85.
20 Livak KJ, Schmittgen TD. Analysis of relative gene expression data using real-time quantitative PCR and the 2(-Delta Delta C(T)) Method. *Methods* 2001; **25**: 402–8.
21 Laemmli UK. Cleavage of structural proteins during the assembly of the head of bacteriophage T4. *Nature* 1970; **227**: 680–5.
22 Kyhse-Andersen J. Electroblotting of multiple gels: a simple apparatus without buffer tank for rapid transfer of proteins from polyacrylamide to nitrocellulose. *J Biochem Biophys Methods* 1984; **10**: 203–9.
23 Clauss A. Rapid physiological coagulation method in determination of fibrinogen. *Acta Haematol* 1957; **17**: 237–46.
24 Aden DP, Fogel A, Plotkin S *et al.* Controlled synthesis of HBsAg in a differentiated human liver carcinoma-derived cell line. *Nature* 1979; **282**: 615–16.
25 Knowles BB, Howe CC, Aden DP. Human hepatocellular carcinoma cell lines secrete the major plasma proteins and hepatitis B surface antigen. *Science* 1980; **209**: 497–9.
26 Baumann H, Won KA, Jahreis GP. Human hepatocyte-stimulating factor-III and interleukin-6 are structurally and immunologically distinct but regulate the production of the same acute phase plasma proteins. *J Biol Chem* 1989; **264**: 8046–51.
27 Kosuge M, Takizawa H, Maehashi H *et al.* A comprehensive gene expression analysis of human hepatocellular carcinoma cell lines as components of a bioartificial liver using a radial flow bioreactor. *Liver Int* 2007; **27**: 101–8.
28 Japanese Collection of Research Bioresources Cell Bank. Available at: http://cellbank.nibio.go.jp/~cellbank/en/search_res_det.cgi?ID=2136. Accessed April 6, 2014.
29 Mooney D, Hansen L, Vacanti J *et al.* Switching from differentiation to growth in hepatocytes: control by extracellular matrix. *J Cell Physiol* 1992; **151**: 497–505.
30 Fish RJ, Neerman-Arbez M. Fibrinogen gene regulation. *Thromb Haemost* 2012; **108**: 419–26.
31 Clevenger FW. Nutritional support in the patient with the systemic inflammatory response syndrome. *Am J Surg* 1993; **165**: 68S–74S.
32 Semenza GL. Defining the role of hypoxia-inducible factor 1 in cancer biology and therapeutics. *Oncogene* 2010; **29**: 625–34.
33 Mosesson MW. Fibrinogen heterogeneity. *Ann N Y Acad Sci* 1983; **408**: 97–113.
34 Farrell DH, Huang S, Davie EW. Processing of the carboxyl 15-amino acid extension in the alpha-chain of fibrinogen. *J Biol Chem* 1993; **268**: 10351–5.
35 Blobel G, Dobberstein B. Transfer of proteins across membranes. I. Presence of proteolytically processed and unprocessed nascent immunoglobulin light chains on membrane-bound ribosomes of murine myeloma. *J Cell Biol* 1975; **67**: 835–51.
36 Watt KW, Cottrell BA, Strong DD *et al.* Amino acid sequence studies on the alpha chain of human fibrinogen. Overlapping sequences providing the complete sequence. *Biochemistry* 1979; **18**: 5410–16.
37 Kelly JH, Darlington GJ. Modulation of the liver specific phenotype in the human hepatoblastoma line Hep G2. *In Vitro Cell Dev Biol* 1989; **25**: 217–22.
38 Farrell DH, Mulvihill ER, Huang SM *et al.* Recombinant human fibrinogen and sulfation of the gamma' chain. *Biochemistry* 1991; **30**: 9414–20.
39 Roy SN, Procyk R, Kudryk BJ *et al.* Assembly and secretion of recombinant human fibrinogen. *J Biol Chem* 1991; **266**: 4758–63.
40 Binnie CG, Hettasch JM, Strickland E *et al.* Characterization of purified recombinant fibrinogen: partial phosphorylation of fibrinopeptide A. *Biochemistry* 1993; **32**: 107–13.
41 Tojo N, Miyagi I, Miura M *et al.* Recombinant human fibrinogen expressed in the yeast Pichia pastoris was assembled and biologically active. *Protein Expr Purif* 2008; **59**: 289–96.
42 Rudd PM, Elliott T, Cresswell P *et al.* Glycosylation and the immune system. *Science* 2001; **291**: 2370–6.
43 Weisel JW. Structure of fibrin: impact on clot stability. *J Thromb Haemost* 2007; **5** (Suppl 1): 116–24.

HEPATOLOGY
Official Journal of the American Association for the Study of Liver Diseases

Cyclosporin A and Its Analogs Inhibit Hepatitis B Virus Entry Into Cultured Hepatocytes Through Targeting a Membrane Transporter, Sodium Taurocholate Cotransporting Polypeptide (NTCP)

Koichi Watashi,[1] Ann Sluder,[2] Takuji Daito,[1,2] Satoko Matsunaga,[3] Akihide Ryo,[3] Shushi Nagamori,[4] Masashi Iwamoto,[1] Syo Nakajima,[1] Senko Tsukuda,[1,5] Katyna Borroto-Esoda,[2] Masaya Sugiyama,[6] Yasuhito Tanaka,[7] Yoshikatsu Kanai,[4] Hiroyuki Kusuhara,[8] Masashi Mizokami,[6] and Takaji Wakita[1]

Chronic hepatitis B virus (HBV) infection is a major public health problem worldwide. Although nucleos(t)ide analogs inhibiting viral reverse transcriptase are clinically available as anti-HBV agents, emergence of drug-resistant viruses highlights the need for new anti-HBV agents interfering with other targets. Here we report that cyclosporin A (CsA) can inhibit HBV entry into cultured hepatocytes. The anti-HBV effect of CsA was independent of binding to cyclophilin and calcineurin. Rather, blockade of HBV infection correlated with the ability to inhibit the transporter activity of sodium taurocholate cotransporting polypeptide (NTCP). We also found that HBV infection-susceptible cells, differentiated HepaRG cells and primary human hepatocytes expressed NTCP, while nonsusceptible cell lines did not. A series of compounds targeting NTCP could inhibit HBV infection. CsA inhibited the binding between NTCP and large envelope protein *in vitro*. Evaluation of CsA analogs identified a compound with higher anti-HBV potency, having a median inhibitory concentration <0.2 μM. *Conclusion*: This study provides a proof of concept for the novel strategy to identify anti-HBV agents by targeting the candidate HBV receptor, NTCP, using CsA as a structural platform. (HEPATOLOGY 2014;59:1726-1737)

Hepatitis B virus (HBV) infection is a substantial public health problem, affecting ~350 million people worldwide.[1-3] HBV-infected patients have an elevated risk for developing liver cirrhosis and hepatocellular carcinoma. Currently, clinical treatment for HBV infection includes interferon alpha (IFN-α) and nucleos(t)ide analogs. IFN-α therapy yields long-term clinical benefit in only less than 40% of patients and can cause significant side effects. Nucleos(t)ide analog treatment can suppress HBV replication and is accompanied by substantial biochemical and histological improvement; however, it may select for drug-resistant viruses, which limit the efficacy of long-term treatment. To overcome these problems, the development of new anti-HBV agents targeting a different step of the HBV life cycle is urgently needed.

As HBV has only one viral gene encoding an enzymatic activity, the polymerase, there is no apparent strategy to develop a new class of antiviral agents other than polymerase inhibitors. Hence, it is important to define alternative molecular targets for anti-HBV agents as well as to identify potential anti-HBV

Abbreviations: CN, calcineurin; CsA, cyclosporin A; CyPs, cyclophilins; HBs, viral envelope protein; HBV, hepatitis B virus; HCV, hepatitis C virus; HCVpp, HCV pseudoparticles; IFN, interferon; LHBs, large envelope protein; MDR, multidrug resistance; MHBs, middle envelope protein; MRP, MDR-related protein; NTCP, sodium taurocholate cotransporting polypeptide; PHH, primary human hepatocytes; PPIase, peptidyl prolyl cis/trans-isomerase; SHBs, small envelope protein; TCA, taurocholic acid; TUDCA, tauroursodeoxycholic acid.

From the [1]Department of Virology II, National Institute of Infectious Diseases, Tokyo, Japan; [2]SCYNEXIS, Inc., Durham, NC, USA; [3]Department of Microbiology, Yokohama City University School of Medicine, Yokohama, Japan; [4]Osaka University Graduate School of Medicine, Osaka, Japan; [5]Micro-signaling Regulation Technology Unit, RIKEN Center for Life Science Technologies, Wako, Japan; [6]Research Center for Hepatitis and Immunology, National Center for Global Health and Medicine, Ichikawa, Japan; [7]Department of Virology and Liver Unit, Nagoya City University Graduate School of Medicinal Sciences, Nagoya, Japan; [8]University of Tokyo Graduate School of Pharmaceutical Sciences, Tokyo, Japan.

Received July 25, 2013; accepted December 17, 2013.

Partly supported by grants-in-aid from the Ministry of Health, Labor, and Welfare, Japan, from the Ministry of Education, Culture, Sports, Science, and Technology, Japan, and from Japan Society for the Promotion of Science.

compounds.[3,4] Myrcludex-B is a peptide mimicking pre-S1, which is crucial for the virus-cell membrane interaction. Pretreatment with this peptide has been shown to prevent virus entry and spread of virus infection.[5,6] Phenylpropenamide derivatives and heteroarylpyrimidines (HAP) suppressed HBV replication through capsid disassembly.[7-10] Although the development of the former was discontinued because of significant toxicity,[3] HAP exhibited anti-HBV efficacy in the absence of robust toxicity.[8,10] Deoxynojirimycin derivatives are iminosugars that inhibit alpha-glucosidases. Although treatment with these compounds suppressed HBV secretion in both cell culture and mouse models,[11,12] further investigation will be required to assess their anti-HBV efficacy and the specificity to HBV. Thus, it is an attractive strategy to identify a cellular factor that is specifically involved in HBV infection and relevant for the development of anti-HBV agents.

Cyclosporin A (CsA) is an immunosuppressant clinically used for suppression of the immunological failure of xenograft tissues. CsA primarily targets cellular peptidyl prolyl cis/trans-isomerase (PPIase) cyclophilins (CyPs).[13] The resultant CsA/CyP complex subsequently binds to and inhibits calcineurin (CN), a phosphatase that dephosphorylates nuclear factor of activated T cell (NF-AT) to allow nuclear translocation and transactivation of downstream genes. This CN inhibition contributes to the suppression of immune responses. In addition, CsA is known to inhibit the transporter activity of membrane transporters, including the multidrug resistance (MDR) and MDR-related protein (MRP) families.[14] Previously, we demonstrated that CsA and its nonimmunosuppressive derivatives suppress hepatitis C virus (HCV) replication,[15,16] with the anti-HCV activity being mediated by the inhibition of CyPs.[17-19] Currently, a series of drugs classified as CyP inhibitors are in clinical development for treatment of HCV-infected patients.[20,21]

In this study we report that CsA and its analogs inhibited HBV entry through a CyP-independent mechanism. We established a screening system that can identify small molecules inhibiting HBV entry. Screening in this system revealed that CsA blocked HBV entry. The anti-HBV activity of CsA was not correlated with binding to CyPs and CN. CsA inhibited the transporter activity of sodium taurocholate cotransporting polypeptide (NTCP), a recently reported candidate for the HBV entry receptor,[22] and interrupted the binding between NTCP and large envelope protein *in vitro*. Other NTCP inhibitors also blocked HBV infection. Analog testing identified CsA-related compounds with higher anti-HBV potency than CsA. Thus, CsA and NTCP inhibitors can be used as a platform to develop a novel class of anti-HBV agents.

Materials and Methods

Cell Culture. HepaRG (Biopredic), HepAD38 (kindly provided by Dr. Christoph Seeger at Fox Chase Cancer Center), and primary human hepatocytes (PHHs) (Phoenixbio) were cultured as described previously.[23]

HBV Preparation and Infection. The HBV used in this study was mainly derived from the culture supernatant of HepAD38 cells. HBV infection was performed as described previously.[23] More detailed procedures are given in the Supporting Information.

Indirect Immunofluorescence Analysis, Real-Time Polymerase Chain Reaction (PCR), Southern Blot Analysis, 3-(4,5-Dimethylthiazol-2-yl)−2,5-diphenyltetrazolium Bromide (MTT) Assays, and Reporter Assays. Indirect immunofluorescence analysis, real-time PCR, southern blot analysis, MTT assays, and reporter assays were performed essentially as described.[23] More detailed procedures are given in the Supporting Information.

Detection of HBs and HBe Antigens. HBs antigen was quantified by enzyme-linked immunosorbent assay (ELISA) as described previously.[23] HBe antigen was detected by a Chemiluminescent Immuno-Assay (Mitsubishi Chemical Medience).

HCV Pseudoparticle Assay. The HCV pseudoparticles (HCVpp), which reproduce HCV envelope-mediated entry, were generated by transfecting the

Address reprint requests to: Koichi Watashi, Ph.D., Department of Virology II, National Institute of Infectious Diseases, 1-23-1 Toyama, Shinjuku-ku, Tokyo, 162-8640, Japan. E-mail: kwatashi@nih.go.jp; fax: +81-3-5285-1161.

View this article online at wileyonlinelibrary.com.

DOI 10.1002/hep.26982

Potential conflict of interest: A.S., T.D., and K.B.E. are employees of SCYNEXIS, Inc. Y.T. is on the speakers' bureau for and received grants from Bristol-Myers Squibb and Chugai.

Additional Supporting Information may be found in the online version of this article.

expression plasmids for MLV Gag-Pol, HCV E1E2, and a luciferase that can be packaged into the virion (kindly provided by Dr. Francois-Loic Cosset at the University of Lyon) into 293T cells. HCVpp recovered from the culture supernatant of transfected cells were used in a HCV entry assay as described previously.[24]

Transporter Assay. The transporter activity of NTCP was assayed essentially as described[25] using 293 (Sekisui Medical) and HepG2 cells permanently overexpressing human NTCP. Briefly, the cells were preincubated with compounds at 37°C for 15 minutes and then incubated with radiolabeled substrate, [^{3}H]taurocholic acid (TCA), at 37°C for 5 minutes to allow substrate uptake into the cells. The cells were then washed and lysed to measure the accumulated radioactivity. In this assay, we did not observe cytotoxic effects of compounds at any of the concentrations tested. More detailed procedures are given in the Supporting Information.

AlphaScreen Assay. Recombinant NTCP and HBs proteins, which were tagged with 6xHis and biotin, respectively, were synthesized using a wheat cell-free protein system as described previously.[26] Protein-protein interactions were detected using the AlphaScreen IgG (ProteinA) detection kit (PerkinElmer) according to the manufacturer's instruction. Briefly, the recombinant tagged proteins were incubated with streptavidin-coated donor beads and anti-6xHis antibody-conjugated acceptor beads that generate a luminescence signal when brought into proximity by binding to interacting proteins. Luminescence was analyzed with the AlphaScreen detection program of an Envision spectrophotometer (PerkinElmer). More detailed procedures for the AlphaScreen assay are described in the Supporting Information.

Additional experimental procedures are included in the Supporting Information.

Results

Cyclosporin A Blocked HBV Infection. We focused on HBV entry and established a cell culture system to evaluate this step in HBV infection. To identify small molecules inhibiting HBV entry, we pretreated HepaRG cells[27] with compounds for 2 hours, then added a HBV inoculum and continued incubation with compounds for 16 hours (Fig. 1A). After washing out free HBV and compounds, the cells were cultured for an additional 12 days in the absence of compounds (Fig. 1A). For robust chemical screening, HBV infection was monitored by the viral envelope protein (HBs) level secreted from the infected cells at 12 days postinfection by ELISA. This assay could identify heparin, an HBV attachment inhibitor,[28,29] and bafilomycin A1, a v-type H^+ ATPase inhibitor that blocks acidification of vesicles and HBV entry,[30] but not lamivudine, a reverse transcriptase inhibitor,[31] as compounds reducing HBs protein level in the medium (Fig. 1B). In addition, use of an anti-HBs antibody to neutralize viral entry, but not use of an anti-FLAG antibody, reduced viral protein secreted from the HBV-infected cells (Fig. 1B). Thus, this system is likely to evaluate the effect of compounds on the early phase of the HBV life cycle, including attachment and entry, but not effects on HBV replication. A chemical screen with this system revealed that CsA reduced HBs secretion from HBV-infected cells (Fig. 1B). Treatment with CsA significantly decreased HBc protein expression (Fig. 1C) and HBV DNA as well as cccDNA (Fig. 1D) in the cells and HBe in the medium (Fig. 1E), without causing cytotoxicity (Supporting Fig. S1A). This effect of CsA was not limited to infection of HepaRG cells, as we observed a similar anti-HBV effect of CsA for PHHs (Fig. 1F). The anti-HBV effect of CsA was also observed on HBV infection of PHHs in the absence of PEG8000 (Fig. S1B), indicating that the effect of CsA did not depend on PEG8000, which was normally included in the HBV infection experiments. These data suggest that CsA blocked HBV infection.

Effect of Cyclosporin A on HBV Entry. CsA decreased HBs and HBe secreted from the infected cells in a dose-dependent manner (Fig. 2A). We next investigated which step in the HBV life cycle was blocked by CsA. The HBV life cycle can be divided into two phases: the early phase of infection including attachment, entry, nuclear import, and cccDNA formation, and the following late phase representing HBV replication that includes transcription, assembly, reverse transcription, and viral release.[32] Lamivudine drastically decreased HBV DNAs in HepAD38 cells,[33] which reproduce HBV replication but not the early phase of infection (Fig. 2B). In addition, continuous treatment with lamivudine as well as entecavir and interferon-α for 4 days after HBV infection could decrease HBV DNA levels in HBV-infected HepaRG cells, which suggests an inhibition of HBV replication (Fig. 2C). Nevertheless, lamivudine did not show an anti-HBV effect when applied only prior to and during HBV infection (Fig. 1A,B), suggesting that the anti-HBV compounds identified in Fig. 1A interrupted the early phase of the HBV life cycle.

We then examined whether CsA inhibited attachment or entry. For evaluating HBV attachment,[34] cell surface HBV DNA was extracted and quantified from HepaRG cells exposed to HBV at 4°C for 3 hours and

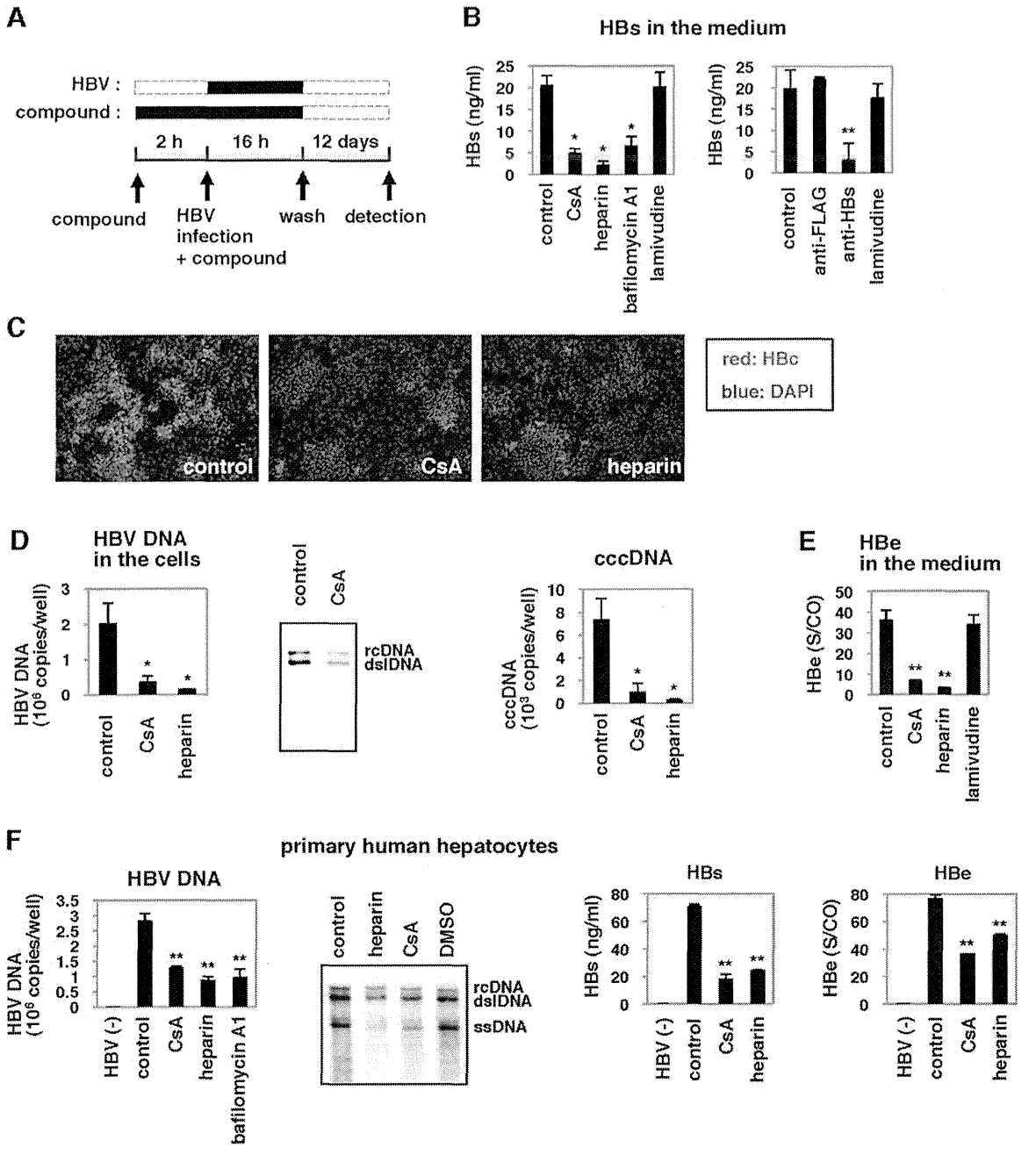

Fig. 1. Cyclosporin A (CsA) blocked HBV infection. (A) Schematic representation of the schedule for exposing HepaRG cells to compounds and HBV. HepaRG cells were pretreated with compounds for 2 hours and then inoculated with HBV for 16 hours. After washing out the free HBV and compounds, the cells were cultured with the medium in the absence of compounds for an additional 12 days to quantify HBs protein secreted from the infected cells into the medium. Black and dotted bars indicate the interval for treatment and without treatment, respectively. (B) CsA 4 μM, heparin 25 U/mL, bafilomycin A1 200 nM, lamivudine 1 μM, anti-FLAG 10 μg/mL, and anti-HBs antibody 10 μg/mL, were tested for effect on HBV infection according to the protocol shown in (A). (C-E) HBc protein (C), HBV DNAs, and cccDNA (D) in the cells as well as HBe antigen in the medium (E) at 12 days postinfection according to the protocol shown in (A) were detected by immunofluorescence, real-time PCR analysis, southern blot, and ELISA. Red and blue in (C) show the detection of HBc protein and nuclear staining, respectively. (F) PHHs were treated with the indicated compounds and infected with HBV using the protocol shown in (A). The levels of HBV DNAs in the cells, as well as of HBs and HBe antigens in the medium, were determined. Statistical significance was determined using the Student t test (*$P < 0.05$, **$P < 0.01$).

then washed (Fig. 2D-a). For the internalization assay,[34] the above cells, after washing, were further cultured at 37°C for 16 hours to allow HBV to internalize into the cells, and then trypsinized to digest HBV remaining on the cell surface to allow quantification of internalized HBV DNA (Fig. 2D-b). CsA slightly reduced the amount of attached HBV DNA, although the effect was not statistically significant